# AFRL-ML-WP-TP-2007-431

# MECHANICAL AND MICROSTRUCTURAL EFFECTS OF COLD SPRAY ALUMINUM ON Al 7075 USING KINETIC METALLIZATION AND COLD SPRAY PROCESSES (PREPRINT)

**John Barnes, Victor Champagne, Donna Ballard, Timothy J. Eden, Brent Shoffner, John K. Potter, and Douglas E. Wolfe**

**JANUARY 2007**

STINFO COPY

**MATERIALS AND MANUFACTURING DIRECTORATE**
**AIR FORCE RESEARCH LABORATORY**
**AIR FORCE MATERIEL COMMAND**
**WRIGHT-PATTERSON AIR FORCE BASE, OH 45433-7750**

# REPORT DOCUMENTATION PAGE

*Form Approved*
*OMB No. 0704-0188*

The public reporting burden for this collection of information is estimated to average 1 hour per response, including the time for reviewing instructions, searching existing data sources, searching existing data sources, gathering and maintaining the data needed, and completing and reviewing the collection of information. Send comments regarding this burden estimate or any other aspect of this collection of information, including suggestions for reducing this burden, to Department of Defense, Washington Headquarters Services, Directorate for Information Operations and Reports (0704-0188), 1215 Jefferson Davis Highway, Suite 1204, Arlington, VA 22202-4302. Respondents should be aware that notwithstanding any other provision of law, no person shall be subject to any penalty for failing to comply with a collection of information if it does not display a currently valid OMB control number. **PLEASE DO NOT RETURN YOUR FORM TO THE ABOVE ADDRESS**.

| 1. REPORT DATE *(DD-MM-YY)* | 2. REPORT TYPE | 3. DATES COVERED *(From - To)* |
|---|---|---|
| January 2007 | Journal Article Preprint | |

**4. TITLE AND SUBTITLE**

MECHANICAL AND MICROSTRUCTURAL EFFECTS OF COLD SPRAY ALUMINUM ON AI 7075 USING KINETIC METALLIZATION AND COLD SPRAY PROCESSES (PREPRINT)

**5a. CONTRACT NUMBER**
In-house

**5b. GRANT NUMBER**

**5c. PROGRAM ELEMENT NUMBER**
62102F

**6. AUTHOR(S)**

John Barnes (Lockheed Martin Aeronautics)
Victor Champagne (US Army Research Lab)
Donna Ballard (AFRL/MLLMP)
Timothy J. Eden, Brent Shoffner, John K. Potter, and Douglas E. Wolfe (The Pennsylvania State University)

**5d. PROJECT NUMBER**
4347

**5e. TASK NUMBER**
RG

**5f. WORK UNIT NUMBER**
M02R2000

**7. PERFORMING ORGANIZATION NAME(S) AND ADDRESS(ES)**

Lockheed Martin Aeronautics
Marietta, GA
------------------------------------
US Army Research Lab
Aberdeen, MD

Metals Branch, Processing Section (AFRL/MLLMP)
Metals, Ceramics, and Nondestructive Evaluation Division
Materials and Manufacturing Directorate
Air Force Research Laboratory, Air Force Materiel Command
Wright-Patterson Air Force Base, OH  45433-7750
--------------------------------------------------------------------------------
The Pennsylvania State University
Applied Research Laboratory
State College, PA

**8. PERFORMING ORGANIZATION REPORT NUMBER**
AFRL-ML-WP-TP-2007-431

**9. SPONSORING/MONITORING AGENCY NAME(S) AND ADDRESS(ES)**

Materials and Manufacturing Directorate
Air Force Research Laboratory
Air Force Materiel Command
Wright-Patterson AFB, OH 45433-7750

**10. SPONSORING/MONITORING AGENCY ACRONYM(S)**
AFRL-ML-WP

**11. SPONSORING/MONITORING AGENCY REPORT NUMBER(S)**
AFRL-ML-WP-TP-2007-431

**12. DISTRIBUTION/AVAILABILITY STATEMENT**
Approved for public release; distribution unlimited.

**13. SUPPLEMENTARY NOTES**
Journal article submitted to the Journal of Thermal Spray and the Journal of Surface Coatings and Technologies.
The U.S. Government is joint author of this work and has the right to use, modify, reproduce, release, perform, display, or disclose the work.  PAO Case Number: AFRL/WS 07-0231, 05 Feb 2007. This paper contains color content.

**14. ABSTRACT**

The objective of this study was to examine how the deposition of a thin layer of Commercially Pure (CP) Al on thin plates of Al-7075 T6 affects the tensile properties of the substrate.  The CP Al was deposited using both Cold Spray and Kinetic Metallization.  Cold Spray utilizes both He and N2 as the carrier gas and a supersonic nozzle while Kinetic Metallization uses only He as the carrier gas and a sonic or friction compensated nozzle.  A test matrix was established to evaluate the coatings applied by both methods.  Characterization of the coatings included microstructural analysis, hardness measurements, and tensile, S-N fatigue and bend tests.  Results of the characterization are presented.

**15. SUBJECT TERMS**
Cold spray, Aluminum, Al 7075, Kinetic Metallization

**16. SECURITY CLASSIFICATION OF:**

| a. REPORT | b. ABSTRACT | c. THIS PAGE |
|---|---|---|
| Unclassified | Unclassified | Unclassified |

**17. LIMITATION OF ABSTRACT:**
SAR

**18. NUMBER OF PAGES**
30

**19a. NAME OF RESPONSIBLE PERSON** (Monitor)
Donna Ballard

**19b. TELEPHONE NUMBER** *(Include Area Code)*
N/A

**Standard Form 298 (Rev. 8-98)**
Prescribed by ANSI Std. Z39-18

# Mechanical and Microstructural Effects of Cold Spray Aluminum on Al 7075 using Kinetic Metallization and Cold Spray Processes

**John Barnes**
Lockheed Martin Aeronautics, Marietta, Georgia, USA

**Victor Champagne**
US Army Research Lab, Aberdeen, Maryland, USA

**Donna Ballard**
USAF Research Lab, Dayton, Ohio, USA

**Timothy J. Eden, Brent Shoffner, John K. Potter, Douglas E. Wolfe**
Applied Research Laboratory, The Pennsylvania State University, State College, Pennsylvania, USA

## Abstract

The objective of this study was to examine how the deposition of a thin layer of Commercially Pure (CP) Al on thin plates of Al-7075 T6 affects the tensile properties of the substrate.  The CP Al was deposited using both Cold Spray and Kinetic Metallization.  Cold Spray utilizes both He and $N_2$ as the carrier gas and a supersonic nozzle while Kinetic Metallization uses only He as the carrier gas and a sonic or friction compensated nozzle.  A test matrix was established to evaluate the coatings applied by both methods.  Characterization of the coatings included microstructural analysis, hardness measurements, and tensile, S-N fatigue and bend tests.  Results of the characterization are presented.

## 1.0  Introduction

The cold spray process technology was originally developed at the Institute of Theoretical and Applied Mechanics of the Siberian Division of the Russian Academy of Science in

Novosibirsk in the mid-1980's, and later patented in the United States in 1994 as part of U.S. interest in Russian Technology [1]. Since then, the cold spray process has been referred to as cold-gas dynamic-spray (CGDS) [2], high velocity particle consolidation (HVPC) [3], cold gas spray (CGS) [4-5], and kinetic spray (KS) [6-7]. Anatoli Papyrin, the inventor of the cold spray process, along with other researchers have shown that the cold spray technology can be used to apply a wide variety of metallic, dielectric (ceramic), metallic alloys, and mixed combinations on a variety of substrate material [3, 8-11]. In general, thermal spray coating processes are divided into two classifications: (a) temperature-based, where feedstock material is rendered molten (or partially molten) through its introduction into intense heat such as an arc, plasma, or flame prior to impingement onto a substrate (i.e., D-gun, plasma spray, and arc spray processes), and (b) velocity-based processes employing high particle velocities and accelerations, lower particle feedstock material temperatures, and shorter transient times (i.e., cold spray, high-velocity air-fuel (HVAF) and high velocity oxy-fuel (HVOF). In HVAF and HVOF, partial melting of powders may still occur depending on the process parameters. Figure 1 illustrates typical particle velocities and gas temperatures for the primary thermal spray coating processes. As shown in Figure 1, gas temperatures in the cold spray process are the lowest of the thermal spray coating processes, and the feedstock particle velocities are some of the highest. The major difference that separates the cold spray process from the conventional thermal spray coating processes is that during the cold spray process the feedstock material does not become molten or partially molten, and deposits in the solid state due to plastic deformation [12-14].

Figure 2 illustrates the cold spray process, in which compressed gas (typically, air, nitrogen, or helium) at pressures from 1-3 MPa is expanded through a converging-diverging (DeLaval) nozzle where it leaves the nozzle at supersonic speeds (180-1200m/s). Typically, the

powder feedstock is introduced into the gas flow slightly upstream of the converging portion of the nozzle. The expanding gas rapidly accelerates the feedstock powder to very high velocities. Velocities range from 180-1200m/s depending on nozzle design, powder characteristics (i.e., density, type, particle size distribution) gas type ($N_2$, He, air), temperature, and material [3,15]. A gas heater is generally used to increase the gas temperature prior to entering the DeLaval nozzle, and results in increased gas velocity and particle temperature. In general, heating the particle increases the particle's ductility and results in increased deposition efficiencies allowing coatings to build up quicker. Within the diverging portion of the DeLaval nozzle, gas rapidly expands causing the gas temperature to drop. As particles are accelerated, they begin to cool, but since the residence time in the nozzle is short, the particle temperature decrease is relatively small. As the particles impact and bond (plastically deform) to a substrate positioned up to 25.4 mm (stand-off distance) from the exit plane of the nozzle, the coating thickness increases. This stand-off distance can be adjusted to change the width of the coating, deposition rate, and sticking efficiency.

Some limitations of conventional thermal spray processes are addressed by the cold spray process [3]. Due to the high deposition temperature of conventional thermal spray processes, limitations exist with the substrate materials that can be coated. Coating materials that undergo phase transformations, recrystallization, excessive oxidation, and evaporation may be difficult or impossible to apply using conventional thermal spray methods. This is especially true for reactive materials such as titanium. Deformation or increased residual stresses induced by the thermal coefficient of expansion mismatch that develop as the coating and substrate cool down after deposition (or after each spray pass) are common in thermal spray processes. Even if the coating remains attached to the substrate, high residual tensile stresses may cause unacceptable

distortions that significantly weaken the bond strength, accelerate fatigue failures, and introduce microcracking reducing the  coating's performance.  Cold spray addresses some of these issues associated with conventional thermal spray techniques.  The lower deposition temperatures reduce the effects associated with recrystallization in both the substrate and coating.  Oxidation of metallic species is greatly reduced, which generally increases coating performance in corrosion environments.  CS technology can be applied to a wider variety of substrates and residual stresses are generally compressive in nature, due to the physics of the impinging particles.  Thick coatings can readily be built-up making cold spray technology a viable candidate for rapid prototyping.  Noise levels are significantly lower and there are no dangerous metal vapor fumes (however, depending on the size of the powders, necessary precautions should always be taken to prevent inhalation) [3, 8-9].

The present work attempts to describe the effects of cold deposition to a Al 7075 T6 rolled sheet substrate after deposition of CP Al powder via cold spray and Kinetic Metallization™ methods.  Variables considered during the trial are:  Particle velocity, carrier gas and post deposit aging.  Effects were measured through tensile, fatigue initiation and bend tests.  Standard metallography was also conducted including hardness profiles through the cross section.


## 2.0  Experimental

The substrate material used in this investigation was 0.050" thick, Al 7075 T6 rolled sheet material.  The material was chosen for its well documented behavior and also for its relatively poor corrosion performance [REF].  Using the cold spray system at the Ktech Facility in Albuquerque, N.M., various commercially pure aluminum (**XXXXXXX**) coatings were applied on 2" x 2" sections of the 2" x 8" Al 7075 rolled sheet as shown in Figure 3 representing the

gage section of the mechanical specimens.  Two variations of the cold spray process were selected for comparison in order to better understand the effects of using nitrogen and helium gas.  Prior to coating application, the feedstock powder was baked out in an oven at 150$^o$F to remove moisture and improve powder flowability.  The powder was then weighed, and placed in the Praxair model number 1264 HPHV powder feeder.  Prior to spraying the coatings, the Al7075 sheets substrates were grit blasted (TRINCO Dry Blast) using 16 to 20 grit aluminum oxide powder (TRINCO) to remove surface oxides and create a minimum surface finish of approximately R$_a$ equal to 200 microinches (5.08 μm).  In order to increase the mechanical bonding between the cold sprayed coating and the substrate, a minimum surface roughness is desired but depends on substrate hardness. A final ethyl alcohol rinse followed with compressed air drying was performed just prior to coating deposition to minimize contamination.

Kinetic Metallization was performed by Inovati in Santa Barbra, CA. The specifics of the Kinetic Metallization process were not provided and are considered proprietary by Inovati making direct comparison of the cold spray and Kinetic Metallization process difficult. However, attempts were made to relate the parameters of both processes. The cold spray processing parameters for the various commercially pure Aluminum cold sprayed coatings used in this study are listed in Table I.

Several depositions were performed in order to attempt to optimize the deposition conditions of both the cold spray and KM CP Al samples.  As shown in table I, both He and N$_2$ were used as carrier gases for depositing CS coatings to thickness of  0.003" to 0.005", whereas only He carrier gas was used for KM coatings.

After deposition, selective samples were aged at 325ºF for 17 hours and other coupons were left in the as-processed state.  The effect of this age treatment alters the temper of the

Al7075 substrate from T6 to an overage T76 condition. Select coated samples were then tested

using standard ASTM methodology for S-N Fatigue Initiation (ASTM E466), Tension (ASTM

E8) and Bend (ASTM E290). Fatigue initiation test were run at R = 0.1 and σ 35, 40 and 45 ksi,

and bend tests were run where N = 7. The results will be presented along with select

microstructural analysis.


Table 1. Deposition Processing parameters

| Sample Number | Carrier gas | Coating Material | Aging | Coated samples condition | Gas pressure (psi) | Temperature ($^o$C) | Traverse speed (mm/sec-or min) |
|---|---|---|---|---|---|---|---|
| CS1 | He | CP Al | - | T6 | 250 | 350 | 200 |
| CS2 | He | CP Al | 325$^o$F/17hrs | T76 | 250 | 350 | 300 |
| CS3 | $N_2$ | CP Al | - | T6 | 300 | 300 | 50 |
| CS4 | $N_2$ | CP Al | 325$^o$F/17hrs | T76 | 300 | 300 | 50 |
| KM1 | He | CP Al | - | T6 | proprietary | proprietary | proprietary |
| KM2 | He | CP Al | 325$^o$F/17hrs | T76 | proprietary | proprietary | proprietary |


**3.0 Results and Discussion**

There are several factors that contribute to the measured properties of the coated samples,

including particle velocity, particle morphology, particle size distribution, particle properties,

substrate, substrate surface roughness, nozzle design, carrier gas, and post processing, etc. This

study originally intended to attempt to compare the properties of CS and KM coatings.

However, direct comparison of the coating properties was extremely difficult because the

parameters of the KM process were unknown. However, certain conclusions can be made in

regards to the mechanical properties and microstructural features of the coatings.


**3.1 Ultimate Tensile Stress (UTS)**

The results of the tensile tests are shown in Figure 4 and Table II showing the UTS and YS values for the various coated samples CS1-CS4, and KM1-KM2.  Figure 4a compares the ultimate and yield stress for the various coated samples in the "as desposited" condition, whereas Figure 4b shows the UTS and YS after T76 heat treatment.  As shown from Table II, the UTS values for samples C1-C4 were 82.3 ksi +/-0.2, 59.7 ksi +/-0.7, 82.4 ksi +/-0.1, and 64.2 ksi +/-0.8.  The baseline aluminum 7075-T6 and T76 heat treatment UTS values were determined to be 82.1 ksi and 76.6 ksi, respectively.  In both cases, the UTS values in the "as deposited" condition, were similar to the uncoated baseline value, suggesting that no significant effect on the UTS is observed for CS coatings deposited using helium or nitrogen carrier gas.  However, a larger than expected drop in the UTS value was observed for both the $N_2$ and He carrier gas CS coatings (CS2 and CS4), after T76 heat treatment, resulting in a decrease in the UTS values by 22.1% and 27.4%, respectively, for the cold spray coatings deposited using $N_2$ and He carrier gas.  It should be noted that although the tensile specimen shape conformed to the typical ASTM E8 "dogbone" style and the coating covered the gage area, the coating thickness was not taken into account when calculating the yield and failure stresses and may have resulted in slight error.   A slight reduction in the UTS observed  when using helium gas as compared to nitrogen gas.  A reduction in the UTS of coated specimens as compared to the uncoated substrate was also measured after the T76 heat treatment.  A few possible explanations for some of the observed differences were that the "baseline" Al 7075-T6 were not grit blasted prior to property measurement as compared to the CS coatings which were grit blasted prior to coating deposition.  There also may be a velocity regime where the cold spray process imparts beneficial compressive stresses but above which surface damage may occur. The higher velocities achieved when using helium may have damaged the relatively soft aluminum substrate. Finally, if

7

compressive stresses were induced as a result of the cold spray process, they may have been relieved during the the T76 heat treatment, lowering fatigue resistance.

### 3.2 Yield Stress

Similarly, the yield stress was determined for samples C1-C4 were determined to be 59.4+/-0.8, 55.6+/-0.9, 62.7+/-1.2, and 57.3+/-0.3 KSI, respectively as shown in Table II. For comparison, the uncoated aluminum 7075 T6 and T76 heat treatment conditions are 75KSI and 65.4 KSI, respectively. Both the nitrogen and helium carrier gas (C1 and C3) "as deposited" CS coatings showed a reduction in the YS as compared to the uncoated Al 7075 alloy. Similarly, the T76 CS samples C2 and C4 showed a reduction in the YS after the T76 heat treatment, but not as large as those measured in the as sprayed conditions.

Table II. UTS, YS, % Elongation, and Hardness for select cold spray CP aluminum coated Aluminum 7075 samples.

| Sample Number | Carrier gas | Aging | UTS (KSI) | YS (KSI) | % Elongation | Hardness (VHN$_{0.300}$) |
|---|---|---|---|---|---|---|
| B1 | -- | -- | 82.1 | 75.0 | 14.0 | 178.9 |
| B2 | -- | 325$^o$F/17hrs | 76.6 | 65.4 | 10.0 | 162.2 |
| CS1 | He | - | 82.3+/-0.2 | 59.4+/-0.8 | 11.0+/-3.7 | 58.5 |
| CS2 | He | 325$^o$F/17hrs | 59.7+/-0.7 | 55.6+/-0.9 | 7.6+/-0.2 | 59.2 |
| CS3 | N$_2$ | - | 82.4+/-0.1 | 62.7+/-1.2 | 12.0+/-0.7 | 47.7 |
| CS4 | N$_2$ | 325$^o$F/17hrs | 64.2+/-0.8 | 57.3+/-0.8 | 9.9+/-0.07 | 53.3 |

### 3.3 Elongation

Similarly, the percent elongation of samples CS1-CS4 are shown in Table II. The CP Al sample (CS3) sprayed using the N$_2$ carrier gas showed a percent elongation of 12.0% which was higher than that of the CS Al sample (CS1) sprayed using helium (11.0%) as the carrier gas in the as sprayed condition. For reference, the percent elongation reduced from 14.0% to 10.0% for

the uncoated base alloy in the T76 heat condition. The percent elongation was lower for CS2, which was produced using helium gas. The % elongation was found to be 7.6% which was quite low. The variation in the UTS, YS, and percent elongation may be the result of the tremendous plastic deformation and strain hardening resulting in higher strength and hardness but lower ductility[xx]. Other contributing factors would also include, the combined result of coating depostion variations, substrate pre-treatment, variation in coating thickness, surface roughness, and residual stresses.

### 3.4 Average Vicker's Hardness Value

Lastly, the average vickers hardness values were determined for CS1-CS4, and were found to be 58.5 $VHN_{0.300}$, 59.2 $VHN_{0.300}$, 47.7 $VHN_{0.300}$, and 53.3 $VHN_{0.300}$, respectively. The higher average vicker's hardness values for the CS coatings deposited using helium (CS1-CS2) as compared to nitrogen are attributed to the coatings being more dense resulting from the higher particle velocity during impact for the helium carrier gas as compared to the nitrogen carrier gas. Higher particle velocities result in increase particle deformation resulting in increased density and thus hardness. The increase in VHN with T76 ageing is believed to be the result of the combination of residual stress relaxation and further densification.

### 3.5 Fatigue Testing

The fatigue behavior for the baseline Al 7075 T6 and select coated samples is shown in Figure 5. It should be noted that the maximum stress (ksi) were determined based on the substrate thickness, ignoring the thickness of the coating for ease of caluculation. This was done as it was assumed the the substrate was carrying the majority of the load. Fatigue properties are

becoming increasingly important with regards to material systems (i.e., substrate and coating systems). In generally assumed that coatings will result in decreased fatigue properties, but heavily depends on the coating properties, processing and deposition method. Figure 5 shows increased cycles to failure with increasing stress for the various coated samples. From a fatigue initiative perspective, the cold sprayed coupons using $N_2$ carrier gas (CS3-CS4) performed nearly equivalent to the KM coupons using He carrier gas (KM1-KM2). However, the KM samples did not show acceptable adhesion as discussed in the next section; therefore , suggesting that the test measured the fatigue capability of the substrate, since there was no evidence of surface peening and/or damage. Based on mathematic models, cold sprayed coupons using He gas (CS1-CS2) would have resulted in higher impact velocity and consequently greater surface modification and possible damage which may have effected the fatigue properties negatively. However, much further analysis is required before conclusions can be drawn with regards to CS coatings and fatigure properties.

The "as processed" coupons behave as shot peened coupons. The baseline control and coated coupons show good agreement in $F_{TU}$, however the $F_{TY}$ of the coated coupons are suppressed when compared the the control coupons. The decrease in $F_{TY}$ can be related to the deposition process. Prior to coating, the samples were grit blasted to increase surface roughness which results in a higher bond strength. As the particle impacts the roughened substrate, both the substrate and the particles deform creating strain induced residual stresses in the coating and the substrate. The deformation of the particles, and hence, the strain induced stresses increase as the particle velocity increases. Coating hardnesses were 48 $VHN_{0.300}$ for C3 (cold sprayed with $N_2$) and 59 $VHN_{0.300}$ for (C1) the as processed, cold sprayed with He which is consistent with the decrease in $F_{TY}$.

Previous work [11] in this area using the cold spray process also noted suppressed $F_{TU}$ values after annealing although they were primarily evaluating the aluminum coating itself. They went on to deduce that annealing at 626ºF reduces the dislocation density within the aluminum grains and promotes short term diffusion at the grain boundaries. The notable exception is the KM processed samples. The as processed KM coated samples did not adhere well enough to affect the tensile behavior of the coupon. Furthermore, the intensity of the peening may have been lower due to the nozzle design.

After aging, the $F_{TU}$ and $F_{TY}$ have been impacted on both processes. Unless there is an exterior influence not reported, it is surprising that the KM coupons are now showing effects of peening that did not exist in the as processed coupons. Additionally, the KM coupons were aged apart from the other coupons, and the electrical conductivity measurements were slightly higher than the cold sprayed coupons. This is not necessarily conclusive, but could indicate that these samples were aged to a substrate temper of T73 which has inferior properties to T76.

The cold sprayed coupons that were aged, showed a more suppressed $F_{TU}$ and $F_{TY}$ than the control coupons. The electrical conductivity measurements agree with a T76 temper. It is still inconclusive as to why the mechanical properties are inferior to the baseline.


### 3.6  Bend Tests and Adhesion

Bend tests were performed in the as deposited and after T76 heat treatment to determine the influence on adhesion. Figure 6a-6f shows digital images of the post bend test for samples CS1-CS4 and KM1 and KM2, respectively. The bend tests were consistent with the tensile test results and analysis. As shown in Table 3, the bend tests showed that the cold sprayed coatings using the nitrogen carrier gas (C3-C4) resulted in no cracking in the "as deposited" (C3) and T76 heat

treatment (C4) conditions, and thus showed the best performance.  In the present study, all of the

coatings applied using He carrier gas (C1-C2 and KM1-KM2) showed evidence of cracking in

the bend test.  Although one may conclude from the test data that since no cracking was observed

in samples C3-C4 before or after the T76 heat treatment that nitrogen carrier gas resulted in

better adhesion, additional testing is required as the authors do not believe that the spray

parameters were fully optimized for these conditions.  The better adhesion for C3-C4 is

attributed to the deposition parameters being more optimized for nitrogen carrier gas as

compared to helium.  Overall, the aged coupons, as shown in Figure 6 showed better adherance

than the "as deposited" coated coupons suggesting that some metallurgical bonding is taking

place during the T76 heat treatment via thermal transport.  Further investigation is needed to

determine whether peening and compressive residual stresses associated with the CS processes

influences the adhesion of the coatings.

Table 3:  Bend and electrical conductivity test results and qualitative comments of the state of coating after completion.

| Sample Number | Carrier gas | Aging | Coated samples condition | Bend Test Results | Average electrical conductivity (units) |
|---|---|---|---|---|---|
| CS1 | He | - | T6 | Major Cracking | 31.9% |
| CS2 | He | $325^{o}$F/17hrs | T76 | Minor Cracking | 38.5% |
| CS3 | $N_2$ | - | T6 | No Cracking | 32.0% |
| CS4 | $N_2$ | $325^{o}$F/17hrs | T76 | No Cracking | 38.5% |
| KM1 | He | - | T6 | Major Cracking | 32.0% |
| KM2 | He | $325^{o}$F/17hrs | T76 | Major Cracking | 41.0% |

Based on the bending tests, it would appear that the coating adhesion had some dependency

on particle velocity, assuming that the particle velocities using the helium carrier gas was greater

than those using the nitrogen carrier gas.  Preliminary test data seems to suggest that too much

particle velocity or impact energy may be deleterious as can too little. The fatigue, tensile and bend tests were consistent with regards to the coating staying adhered during testing. Specimens aged after deposition also showed increased adherance independent of the other factors. Although the strength of the substrate was lowered through overaging, the coating showed more resilience to cracking during bending and did not spall off as readily as the carrier gas will primarily affect the aluminum powder particle velocity.

**Residual Stress**

The stress of the various coatings was determined using the $\sin^2\Psi$ technique [3.3-3.4] and a Philips X'Pert model MRD. The stress cannot be measured directly by x-ray diffraction. Rather, the strain is measured and the stress is calculated. Strain was determined by measuring the interatomic spacing of a particular set of planes as a function of several $\psi$ tilts (angle of inclination to the surface). By plotting the interatomic spacing as a function of the $\sin^2\psi$, the stress was calculated from the slope and the following equation:

$$\sigma_\phi = (E / (1 + \upsilon))_{(hkl)} \, (1 / d_{\phi o}) \, (\vartheta d_{\phi\psi} / \vartheta \sin^2\psi)$$

Where $\sigma_\phi$ is the stress in the surface direction, E and $\upsilon$ are the elastic modulus and Poisson's ratio, respectively, for the planes of interest, $d_{\phi o}$ is the interatomic spacing at zero tilt, and $\vartheta d_{\phi\psi}$ /$\vartheta \sin^2\psi$ is the slope of the interatomic spacing ($d_{\phi\psi}$) plotted as a function of $\sin^2\psi$. It should be noted that the stress measurements determined by x-ray diffraction assumes a plane stress condition (biaxial stress). During the stress determination, the degree of crystallinity and texturing can influence the stress results and often lead to errors. Prior to performing the x-ray

diffraction residual stress analysis, x-ray diffraction patterns were obtain to ensure no significant crystallographic orientation (i.e., texturing) was observed that would result in increase error in the stress measurements. In addition, in order to determine the amount of residual stress in select coatings, plain strain conditions were assumed. Using the {422} planes of aluminum, the residual stresses were measured. Using $E_{422}$ equal to 70 GPa and a poisons ratio of 0.33, the residual stresses for C1-C4 were determined to be -13.2 MPa +/-1.5, -13.0 MPa +/-0.5, -16.6 MPa +/-2.4, and -18.3 MPa +/-2.7. The negative sign for the residual stress means that the residual stresses in all of the cold spray coatings were compressive resulting from the "peening" effect. The x-ray diffraction residual stress measurements confirm that the CS coatings are in residual compression, and that the substrate must be in residual tension for force balance. When coating is applied to both sides of the sample, a residual stress state as shown in Figure 7 is observed. Although the x-ray diffraction residual stresses measured show that the cold spray coatings using nitrogen carrier gas are slightly more compressive than those sprayed with helium carrier gas, it is unclear as to whether the slight difference is due to the impact energy resulting in increased plastic deformation for the helium carrier gas. It should be noted that the measured residual stresses are elastic, and not plastic. Increased particle velocities may have resulted in increased particle plastic deformation, and thus lower residual compressive stresses as compared to the nitrogen carrier gas.

### 3.7 Electrical Conductivity

In addition, electrical conductivity measurements were made on select samples as listed in Table 3 for the various conditions. The corresponding IACS values to temper are as follows: 33% = T6, 38.5% = T76, 40% = T73 [8]. As observed in Figure 3, the IACS values correspond

to the T76 temper.   The electrical conductivity measurements were made in an effort to determine whether significant changes in the coating microstructure, i.e., density, were occuring during the aging treatments.  In all cases, the average electrical conductivity increases with the T76 heat treatment.


### 3.8  Effect to the Substrate

The bonding mechanism between particles and substrate and between particles and previously deposited particles is caused by substrate penetration, interfacial heating, and liquid jet formation resulting from high-velocity impact.  These phenomena are described by others, where the behavior of a single particle impacting a substrate is modeled [9].  The computation uses the Zerilli-Armstrong (strain-rate dependent) and the Steinberg-Guinan-Lund plastic models, respectively, for copper particles impacting an aluminum plate.  The calculation shows that the interfacial pressure and von Mises equivalent stress are considerably higher than the zero plastic-strain yield strength of copper and aluminum, it is appropriate to treat the material adjacent to the interface as a viscous "fluid-like" material.   The viscous, fluid-like nature of the jet can be expected to result in the formation of interfacial waves, roll-ups and vortices.

Cold spray may act similarly as traditional shot peening does on a smaller scale due to smaller media.  Shot peening is effective in prolonging fatigue life by introducing compressive residual stresses locally at the surface [10].  If the intensity of the peening is too high, the residual stress will become thicker and promote fatigue fracture.  The fatigue life is enhanced by suppressing the yield strength locally.

The two processes and two carrier gases gave insight into the impact energy or peening effect. Each produced a different velocity ranging from 1,300 ft/s to nearly 4,000 ft/s (estimate). The higher the impact energy, the lower the $F_{TY}$ became.

The design of the specimen may also contribute to some of the tensile behavior witnessed in the study. By coating only the gage section, the bulk stiffness of the coupon has been altered which may impact the tensile behavior ($E_{CPAl} = 10.3$ Msi, $E_{7075} = 10.0$ Msi) when compared to the untreated coupons.

The post process aging could be promoting some material transport across the interface. This would support the increased adhesion behavior. Other consequences could result in reducing discloation density and relief of residual stress which will strongly affect the mechanical behavior ($F_{TY}$). If the adhesion is strong enough, cracks in the coating could be driven into the base material which would result in further suppression of the $F_{TU}$.

### 3.9  Conclusion

Based on the preliminary data and results, it is too early to conclude whether either process is capable or incapable of providing a CP Al coating without negatively impacting the mechanical properties. The data does suggest that particle velocity and consequently, the peening intensity must be optimized to balance adhesion, static strength and fatigue life improvement. As expected, post process aging improves coating adhesion, but reduces the strength. Certain aspects of this work should be duplicated in order to discern whether optimization of the deposition parameters can be made to enhance the peening effect and consequently, the mechanical properties and adhesion. Tests should be conducted on uncoated,

gritblasted, coated,  and in both the T6 and T76 conditions.  Residual stress measurements and a more in-depth analysis of the coating/substrate interface is also needed.

**4.0 References**

1.  R.C. Dykhuizen, M.F. Smith, D.L. Gilmore, R.A. Neiser, X. Jiang & S. Sampath, Impact of High Velocity Cold Spray Particles, *J. of Therm. Spray Tech.*, Vol 8 (No 4), 1999.

2.   F.Papyrin: Cold Spray Technology, *Advanced Materials & Processes*, September, 2001, pp. 49 – 51.

3.  R. McCune, W. Donlon, O. Popoola, and E. Cartwright. Characterization of Copper Layers Produced by Cold Gas-Dynamic Spraying, *Journal of Thermal Spray Technology*, 2000, 9 (1), pp. 73 – 82.

4.  T. Stoltenhoff, H. Kreye, and H. Richter. An Analysis of the Cold Spray Process and Its Coatings, *Journal of Thermal Spray Technology*, 2002, 11 (4), pp. 542 – 550.

5.  V. Radic. The State of Two-Metal Contact Boundary at High-Velocity Impact, *The Scientific Journal FACTA UNIVERSITATIS Series: Mechanical Engineering* 2001, 1(8), pp. 1017 – 1023.

6.  W. de Rosset.  Explosive Bonding of Refractory Metal Liners, *ARL-TR-3267*, Army Research Laboratory, Aberdeen Proving Ground, MD, August, 2004.

7.  H. Gabel & R. Tapphorn, Surface Modification by High Speed Macroscopic Particle Impact, *Surface Modification Technologies,* Vol. IX, 1996.

8.   ASM Handbook, Vol. 2, p. 116, 1992.

9.  M. Grujicic, J. Saylor, D. Beasely, W. DeRosset, and D. Helfritch. Computational Analysis of the Interfacial Bonding between Feed-Powder Particles and the Substrate in the Cold-Gas Dynamic-Spray Process, *Applied Surface Science*, 2003, 219(3-4), pp. 211-227.

10. P. Black, Understanding the Beneficial Effects of Shot Peening, *Materials Engineering Quarterly*, Aug. 1972.

11. A.C. Hall, D.J. Cook, R.A. Neiser, &  T.J. Roemer, The effect of a simple annealing heat treatment on the mechanical properties of cold sprayed aluminum, *International Thermal Spray Conference Proceedings*, 1995.
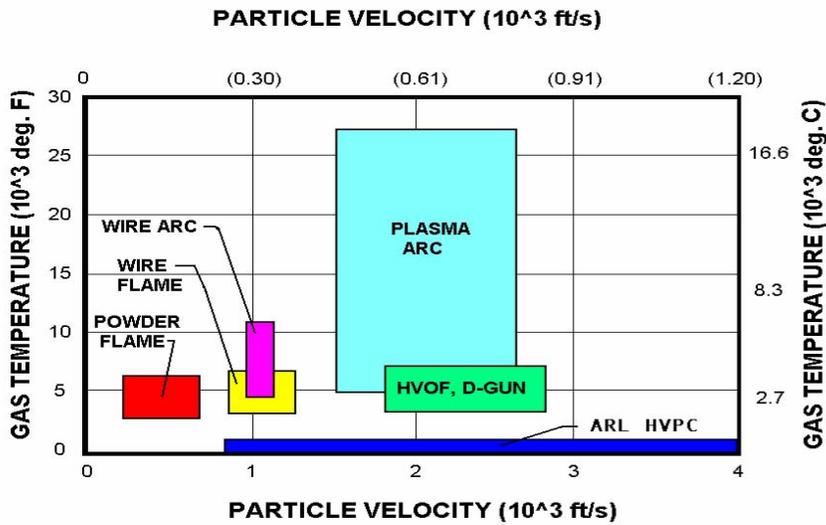
Figure 1.  Graphical representation of the temperature and pressure regimes of the various thermal spray processes including wire arc, wire flame, powder flame, plasma arc, HVOF, D-gun, and Cold spray.
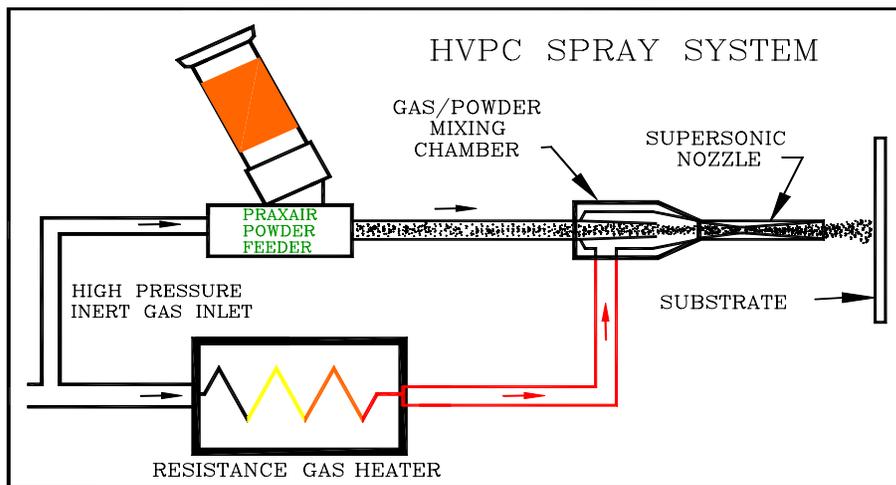


Figure 2.  Schematic drawing of the cold spray process.
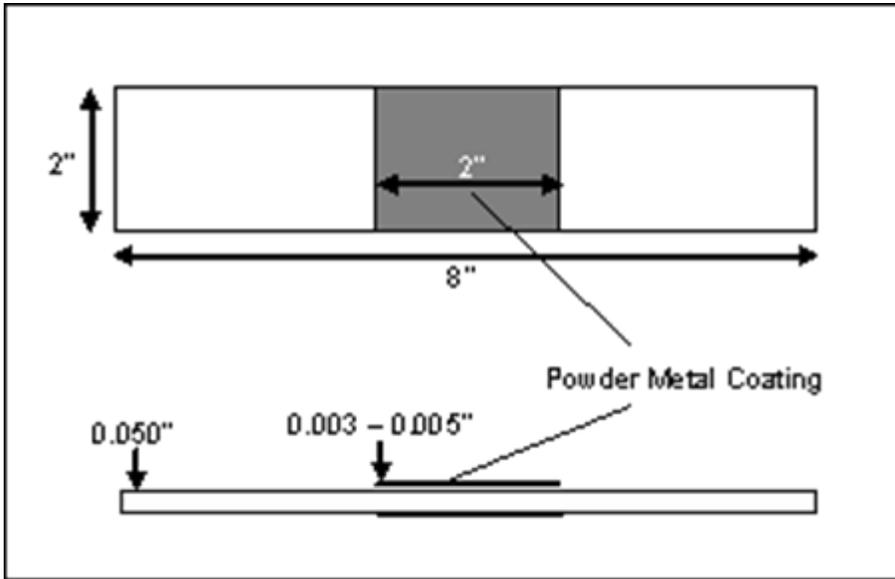
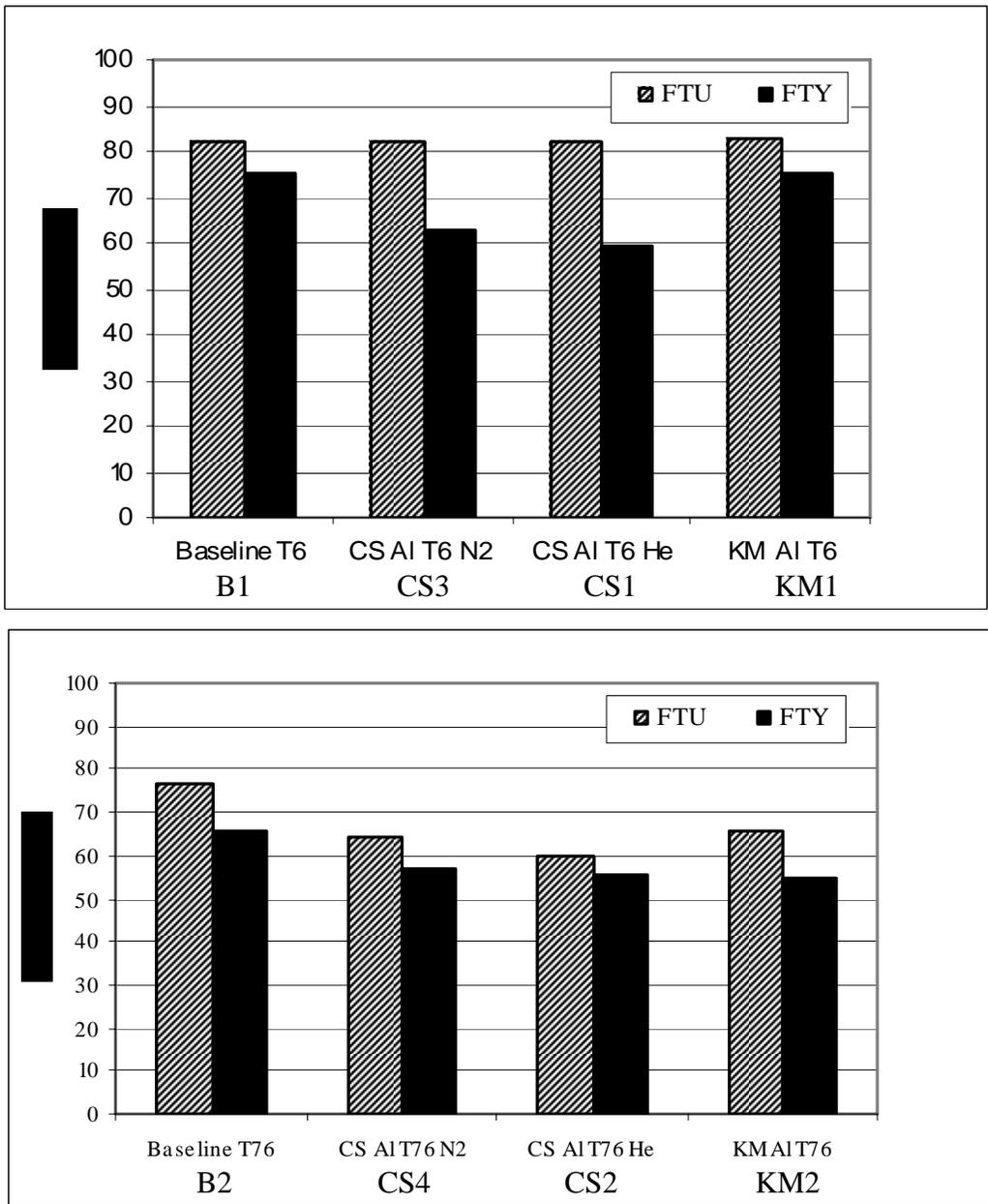Figure 3.  Coated area of the test specimen  and coupon dimensions with coating location and thickness specifics.

Figure 4. UTS and YS results for various baseline and cold sprayed coatings in the
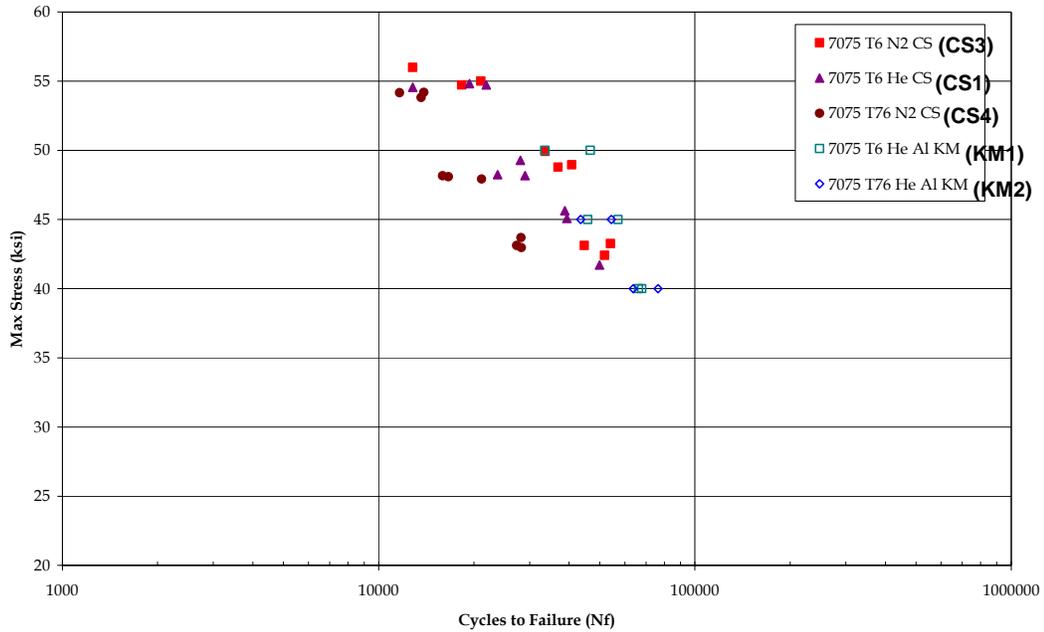(a) "as deposited" (T6) and (b) T76 heat treated conditions.

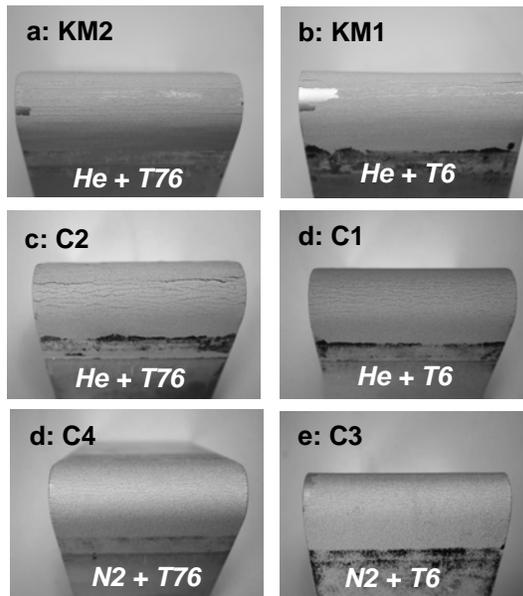Figure 5. Fatigue behavior comparing cold spray, KM and baseline materials.



Figure 6. Digital images of bend test coupons (a) KM2, (b) KM1, (c) C2, (d) C1, (e) C4, and (f) C3 showing cracking for select samples

Coating  Substrate  Coating

Incident powder particles are impacted onto the substrate surface

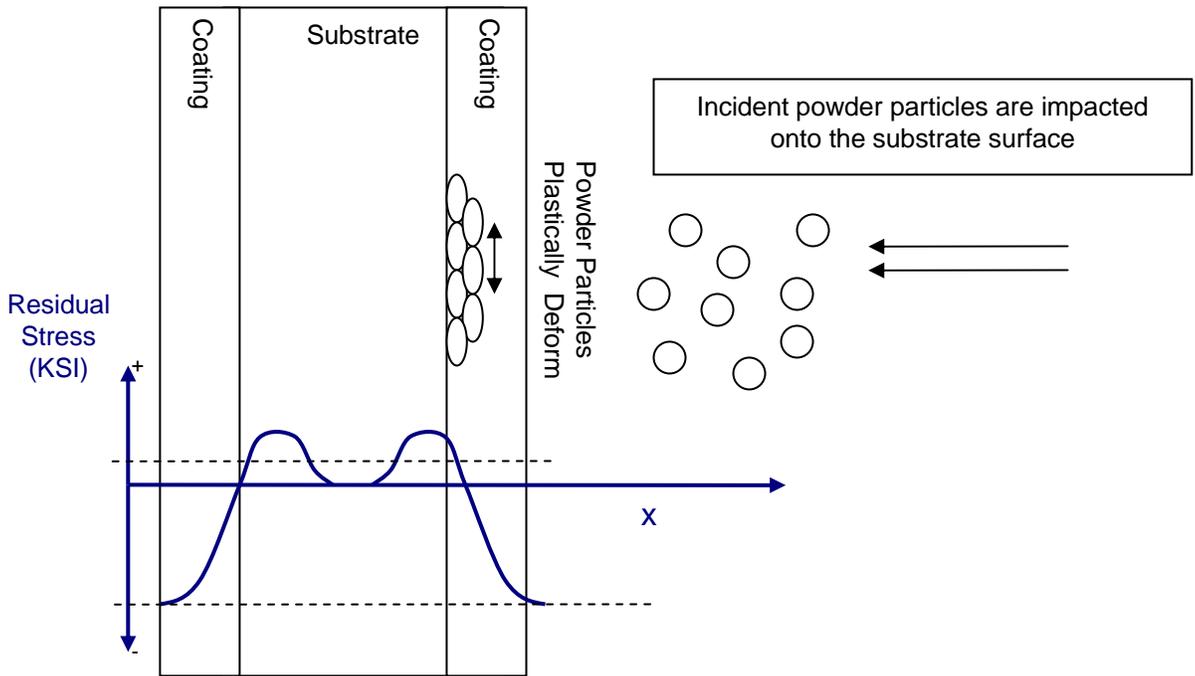Powder Particles Plastically Deform

Residual Stress (KSI)

+

x

-

Figure 7. Schematic representation of impacted particles on coating and substrate residual stresses in cold sprayed coatings.